Proceedings of International Computer Symposium 1994
December 12-15, NCTU, Hsinchu, Taiwan, R.O.C.

Autonomous Land Vehicle Guidance by Line and Road Following Using Clustering, Hough Transform, and Model Matching Techniques

Guang-Shern Cheng(陳光雄) and Wen-Hsiang Tsai(蔡文祥)

Department of Computer and Information Science, National Chiao Tung University, Hsinchu, Taiwan 300, Republic of China

Abstract

An intelligent approach to autonomous land vehicle (ALV) guidance by line and road following using clustering, Hough transform, and model matching techniques is proposed. The purpose of clustering is to separate the road from the other objects in an input image. Then, road-model matching is employed to find the best road-template which can be used to locate the ALV. Moreover, path lines in the matched road are extracted using the Hough transform, and line-model matching is used to find the best line-template which also can be used to locate the ALV. If no line can be found in the road, we use the matched road-template to locate the ALV. But if lines exist, we use them to locate the ALV. Several successful navigations show that the proposed approach is effective for ALV guidance in common roads.

1. Introduction

Many techniques have been proposed and implemented for the ALV guidance. In Ku and Tsai [1], a model-based navigation approach was proposed, and the corridor contour was used as the model. In Cheng and Tsai [2], a new navigation approach by model matching was proposed, where the locations of vertical lines in indoor environments are used as the model. In outdoor environments, VITS [3] and Navlab [4] both use color information in RGB planes for road following. Turk et al. [3] show that the G-component is useless in their road segmentation. Navlab [4] analyzes both the color and texture segmentation results using a standard pattern classification method involving the mean and the covariance matrix. Lin and Chen [5] classified the road into three clusters : sunny road, shadow road and nonroad. Their analysis and classification are based on the KL-transformation in the HSI space. Kluge and Thorpe [6] separated the assumptions made in road modeling into three loose categories: subconscious, implicit and explicit models. Also, a new road tracking system, FERMI, was built to study explicit models and their use. The vision system in Germany [7], [8], [9] can guide the vehicle on an autobahn at speeds up to 100 kph, incorporating a high-speed vision algorithm to track road border lines. The system has performed both road following and vehicle following in real-time. UNSCARF [11] used an unsupervised clustering technique [15] to classify the unstructured road into homogeneous regions. Then, small regions are removed using a shrink and expand algorithm [16]. Finally, a minimum distance criterion is used to find the best candidate interpretation by applying a Grassfire transformation [17]. Kuan, Phipps, and Hsueh [13] proposed a technique with transformation and classifier parameters being updated gradually and cyclically according to the slow change of color and intensity.

In this paper, we propose an intelligent ALV guidance approach which can detect the road and extract the lines on the matched road based on a modified clustering method [15] and the Hough transform [18]. For clustering, we choose the initial cluster centers by analyzing the histograms of the R, G and B planes individually to produce effective clusters. Basically, the road is divided into three clusters: bright cluster, gray cluster and dark one. We perform road-model matching using the gray cluster because it is most likely to be the road area. The Hough transform does not take much computing time because the bright pixels on the matched road are very few (typically, the bright area includes just the yellow lines on the road). Therefore, real-time navigation can be carried out. The proposed approach is proved effective after many practical navigation tests.

The remainder of this paper is organized as follows. The principle of the proposed approach is presented is Section 2. In Section 3, the results of some experiments are described. Finally, some discussions are made in Section 4.

2. Principle of Proposed Research

An overview of the proposed approach is shown in Fig. 1. The details are described in the following.

2.1 Model Creation

Assume that the road boundaries and the lines on the road are straight and parallel to each other, and the surface is earth-flat. We can represent the location of the ALV by (d, θ), where d is the distance of the ALV to the central path line and θ is the pan angle of the ALV relative to the road direction. The equations of the two road boundaries in the vehicle coordination system (VCS) are assumed to be known. Then, we can transform them into the image coordination system (ICS) which is displayed on the TV monitor. Therefore, for each ALV location (d_i, θ_j), we can create its corresponding road-templates ROAD[i][j][a_l, b_l, a_r, b_r], where a_l, a_r are the slopes and b_l, b_r are the intercepts of the equations of the left and right boundaries in the ICS, respectively. The transformation is shown in Fig. 2(a). We divide the road width into 23 positions (position interval = 25 cm). Each position contains 17 pan angles (-16 degree ~ +16 degree, angle interval = 2 degree). So, the road-model contains 23x17=391 road-templates, and each road-template represents one ALV location. We use the same method to create the line-model provided that there are at most three lines (left, middle and right) on the road. The line-model also contains 23x17 line-templates, and each line-template LINE[i][j][a_l, b_l, a_m, b_m, a_r, b_r] also represents an ALV location (d_i, θ_j). The transformation is shown in Fig. 2(b). Thus, each ALV location (d_i, θ_j) can be represented by ROAD[i][j][a_l, b_l, a_r, b_r] or LINE[i][j][a_l, b_l, a_m, b_m, a_r, b_r].

2.2 Color Image Reduction and Clustering

To reduce the image size, the pixels are sampled from the original image with the interval of 5 pixels in both the horizontal and vertical directions, and the upper portion is discarded because it does not contain any road area. For clustering, we use a modified ISODATA algorithm [13], called the ICC (Initial-Center-Choosing) algorithm, to divide the reduced RGB color image into three clusters:

<1> cluster-0: dark area, like the shadows and trees;

<2> cluster-1: gray area, the main body of road;

<3> cluster-2: bright area, like the sky and yellow lines on the road.

The ICC algorithm is described as follows. Assume that we want to divide the road into i clusters. We first observe the histogram of the R-plane, and divide all the pixels into 2i pieces of the same size as shown in Fig. 3, i.e., $\forall\ 0 \le k \le i-1$, we have

$$\sum_{s=r_k}^{r_k'}[pixel\ no.\ of\ g.l.(s)] = \sum_{t=r_k'}^{r_{k+1}}[pixel\ no.\ of\ g.l.(t)] \quad (1)$$

where g. l. means gray level. Then, r_k' is taken to be the R-component of the candidate center of cluster k. Using the same criterion on the G-plane and B-plane, we can find the G-component g_k' and B-component b_k'. We then use $[r_k', g_k', b_k']$ as the initial center of cluster k, k=0, 1, ..., i-1. Comparing with the result which uses gray-level-averaging to set the initial center of cluster k to be

$$\left[\left\lfloor\frac{255}{(i-1)}\right\rfloor * k,\ \left\lfloor\frac{255}{(i-1)}\right\rfloor * k,\ \left\lfloor\frac{255}{(i-1)}\right\rfloor * k\right] \quad (2)$$

as shown in Fig. 4 (c), we can find that the result of the ICC algorithm shown in Fig. 4 (b) is better. These results are obtained by running these two algorithms for 3 cycles. Fig. 5 shows two source images with high intensity and low intensity and the corresponding clustering results in (a) and (b), respectively. It can be seen that the ICC algorithm is not sensitive to the change of intensity. This is another advantage of the ICC algorithm.

2.3 Road-Model Matching

There are two possible criteria for model matching:

<1> maximum-bounded-pixel-number matching (MBPNM):

We define the bounded-area as the area bounded by the two lines of the road-template, and the bounded-pixels as all the pixels belonging to cluster-1 (most likely to be the road area) in the bounded-area. If a road-template includes within its two boundary lines the largest number of bounded-pixels, it can be regarded as the best matched one.

<2>. maximum-bounded-pixel-ratio matching (MBPRM):

We define

maximum bounded pixel ratio
= (bounded-pixels) / (total number of pixels in the bounded area). (3)

Then, a road-model can be considered to be the best matched one if it has the maximum bounded pixel ratio.

The matched road-templates represented by the two red lines using the MBPNM and MBPRM are shown in

Fig. 6. It can be seen that the shadow area is included in (a) and excluded in (b), so we adopt the MBPNM criterion in our approach because the shadow area should be regarded as part of the road. Also, we do not use the entire road-template to do the matching because it waste too much time; we only use the neighboring ones in the model around the reference road-template to perform the matching. The reference road-template is the road-template at the current ALV location which is estimated from the ALV location of the last cycle through control information as shown in Fig. 7.

2.4 Extracting Lines on Matched Road-Template using Hough Transform

After finding out the best road-template, we use the Hough transform to extract the lines in the bounded-area of the matched road-template. This does not take too much time because very few pixels belong to cluster-2 (bright area, typically the yellow lines) in the bounded-area. Furthermore, we search the surrounding area of the three lines of the reference line-template to find the peaks in the ρ-θ Hough counting space to save the computation time, where the reference line-template is the line-template of the current estimated ALV location. We extract at most three lines in the bounded-area to satisfy the assumption, and these lines are taken to match line by line the corresponding lines of the line-templates around the reference-point to find their corresponding best line-templates. Finally, these best line-templates are combined to estimate a reasonable ALV location.

2.5 Line-Model Matching

Without loss of generality, we first take the left extracted line to perform the matching. We want to find the best line-template T_L whose left line is the most similar to the left extracted line. We define

$$\text{similarity} = 1/A, \tag{4}$$

where A=the area bounded by the left extracted line and the left line of the line-template as shown in Fig. 8. Then, the matched line-template $T_L = (d_L, \theta_L)$ has the maximum similarity. If the middle or the right extracted line exists, we can use the same criterion to obtain their corresponding best line-templates $T_M = (d_M, \theta_M)$ and $T_R = (d_R, \theta_R)$, respectively. After the T_L, T_M and T_R are computed, the most meaningful ALV location T can be derived as follows("$\cong$" represents "is similar to"):

if $T_L \cong T_M \cong T_R$, then set
$T=(T_L+T_M+T_R)/3 = ((d_L+d_M+d_R)/3 , (\theta_L+\theta_M+\theta_R)/3)$
else if only $T_i \cong T_j$ ($i \neq j$, i, j= L, M, R), then set
$T=(T_i+T_j)/2 = ((d_i+d_j)/2 , (\theta_i+\theta_j)/2)$
else (T_L, T_M and T_R are not similar to each other) set
$T=T_K$, where T_K is the most similar to the reference line-template, k=L, M, R. (5)

Because there are three lines on the road, we can locate ALV accurately even though there is noise like shadows, people, cars or degraded regions existing on roadsides. If noise appears on the rightside, we can use the left or even the middle line to locate the ALV. Similarly, we can locate the ALV using the right or even the middle line if the noise appears on the leftside. Moreover, if noise exists on both sides, the middle line which is seldom affected by shadows or other noise can be used to locate the ALV. Finally, if no line can be extracted in the road, we can still use the best road-template obtained from the road-model matching to locate the ALV. This flexible process makes the ALV guidance steady.

2.6 Wheel Control

After the most possible ALV location T is found, we choose an appropriate turn angle to guide the ALV closely to the given path. A closeness distance measure from the ALV to the given path is defined to be

$$L_P(\delta) = \left(D_P^F\right)^2 + \left(D_P^B\right)^2 \tag{6}$$

where D_P^F and D_P^B are the corresponding distances from the front and the rear wheels of the ALV to the given path after the ALV traverses a distance S with the turn angle δ as shown in Fig. 9. A smaller value of L_P means that the ALV is closer to the path.

It must be careful that allowing the ALV to turn a larger angle does not mean that better navigation can be achieved. It may cause serious twist. On the other hand, a smaller range of turn angles may cause only a slight closeness to the given path. Thus, there is a tradeoff between smoothness and closeness.

3. Experimental Results

Using the proposed guidance method, a prototype ALV constructed in this study for testing can navigate smoothly along part of the campus road in National Chiao Tung University for about 150m. The width of the road is 6.8 m, and there are three yellow lines on the road. The average speed is 30 cm/sec, and the average cycle time is about 2.1 sec. The ALV can navigate steadily in spite of the fact that there are shades, vehicles, people or degraded regions on the roadsides. It is also not sensitive to sudden changes of intensity because of the effective ICC clustering algorithm from which we can obtain the appropriate clusters after running the algorithm for only three cycles.

4. Discussions

The largest angle allowing the ALV to turn is a tradeoff between the smoothness of navigation and the closeness to the given path. In our experiment, we found through many iterative navigations that a turn from -5 degrees to +5 degrees is a good compromise. Also, we change the power at the right time to make the speed stable on both ascending and descending roads by checking an encoder which can report the distance between two continuous cycles. The road-model and line-model are created based on the assumption that the road boundaries and the lines on the road are straight and parallel to each other. So, when the ALV meets the curved road, it can not navigate regularly because of the violation to the assumption. Guidance on the curved road based on the model matching technique is a good topic for future study. Additionally, the problems caused by the change of sunshine direction, selections of different features on the road and seeking effective algorithms to solve the encountered problems are also future directions of studies.

References

[1] P. Y. Ku and W. H. Tsai, "Model-based guidance of autonomous land vehicle for indoor navigation," *Proc. of Workshop on Computer Vision, Graphics and Image Processing,* Taipei, Taiwan, R.O.C., pp. 165-174, Aug. 1989.

[2] S. D. Cheng and W. H. Tasi, "Model-based guidance of autonomous land vehicle in indoor environments by structured light using vertical line information," *Journal of Electrical Engineering*, Vol.34, No.6, Dec. 1991.

[3] M. A. Turk, D. G. Morgenthaler, K. D. Germban, and M. Marra, "VITS--- a vision system for autonomous land vehicle navigation," *IEEE Trans. on Pattern Analysis and Machine Intelligence*, Vol. 10, No. 3, pp. 342-361, May 1988.

[4] C. Thrope, M. H. Hebert, T. Kanade, and S. A. Shafer, "Vision and navigation for Carnegie-Mellon NAVLAB," *IEEE Trans. on Pattern Analysis and Machine Intelligence*, Vol. 10, No. 3, pp. 362-373, May 1988.

[5] Xueyin Lin and Shaoyun Chen, "Color Image Segmentation Using Modified HSI System for Road Following," *Proc. IEEE International Conference on Robotics and Automation*, Sacramento, CA, U.S.A., April 1991, pp. 1998-2003.

[6] K. Kluge and C. Thorpe, "Explicit Models for Robot Road Following," *Proc. IEEE International Conference on Robotics and Automation*, Scottsdale, AZ, U.S.A., May 1989, pp. 1148-1154.

[7] E. D. Dickmans and A. Zapp, "A curvature-based scheme for improving road vehicle guidance by computer vision," *Proc. SPIE Mobile Robot Conference*, Cambrige, MA, Oct. 1986, pp. 161-168.

[8] K. Kuhnert, "A vision system for real time road and object recognition for vehicle guidance," *Proc. SPIE Mobile Robot Conference,* Cambrige, MA, Oct. 1986, pp. 267-272.

[9] B. Mysliwetz and E. D. Dickmanns, "A vision system with active gaze control for real-time interpretation of well structures dynamic scenes," *Proc. Intelligent Autonomous Systems*, Amsterdam, The Netherlands, Dec. 1986.

[10] Y. Goto and A. Stentz, "The CMU system for mobile robot navigation," *Proc. IEEE International Conference on Robotics and Automation*, Raleigh, NC, U.S.A., pp. 99-105, 1987.

[11] J. D. Crisman and C. E. Thorpe, "UNSCARF, A Color Vision System for the Detection of Unstructured Roads," *Proc. IEEE International Conference on Robotics and Automation*, Sacramento, CA, U.S.A., April 1991, pp. 2496-2501.

[12] R. Wallace, K. Matsuzaki, Y. Goto, and J. Crisman, "Progress in robot road-following," *Proc. IEEE International Conference on Robotics and Automation*, San Francisco, CA, U.S.A., pp. 1615-1621, 1986.

[13] D. Kuan, G. Phipps, and A. Hsueh, "Autonomous Robotic Vehicle Roading Following," *IEEE Trans. on Pattern Analysis and Machine Intelligence*, Vol. 10, No. 4, pp. 648-658, 1988.

[14] A. Waxman, J. LeMoigne, L. Davis, B. Srinivasan, T. Kushner, E. Liang and T. Siddalingaiah, "A visual navigation system for autonomous land vehicle," *IEEE Journal of Robotics and Automation*, Vol. RA-3, pp. 124-141, 1987.

[15] R. Duda and P. Hart, *Pattern Classification and Scene Analysis*, John Wiley and Sons, Inc., 1973.

[16] D. Ballard and C. Brown, *Computer Vision*, Prentice-Hall Inc. 1982.

[17] K. Castleman, *Digit Image Processing*, A. Oppenheim, editor, Prentice-Hall, Inc., 1979.

[18] Rafael C. Gonzalez and Richard E. Wood, *Digit Image Processing*, Addison-Wesley Publishing Company, Inc., 1992.

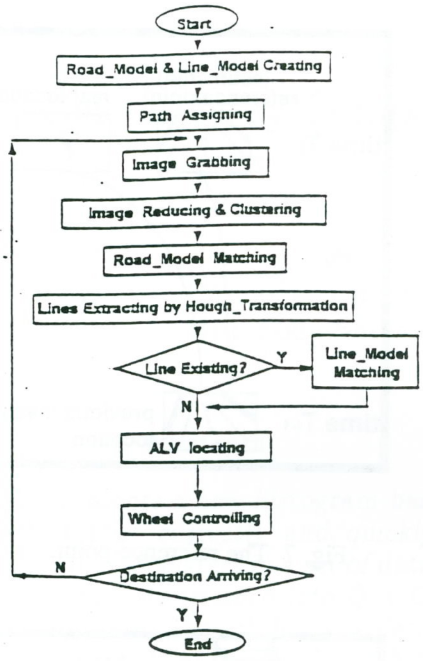

Fig. 1 An overview of the proposed approach.

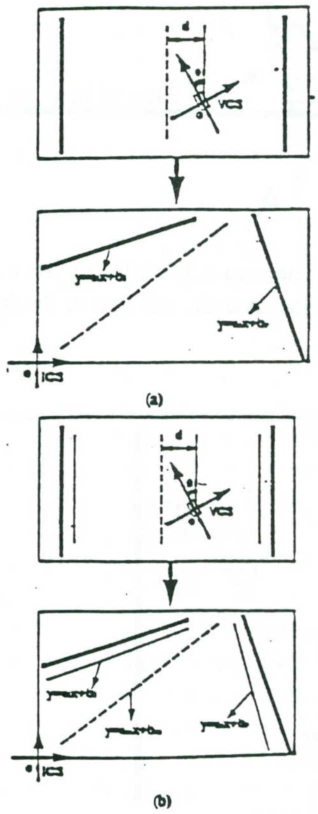

Fig. 2 The transformation between the VCS and the ICS. (a) Road boundary transformation. (b) Line transformation.

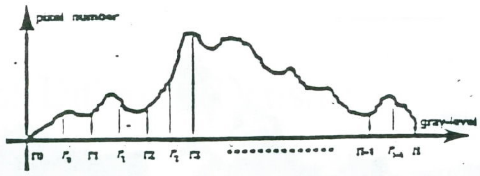

Fig. 3 The histogram of the R-plane where $r_k^{'}$ is the R-component of the center of cluster k.

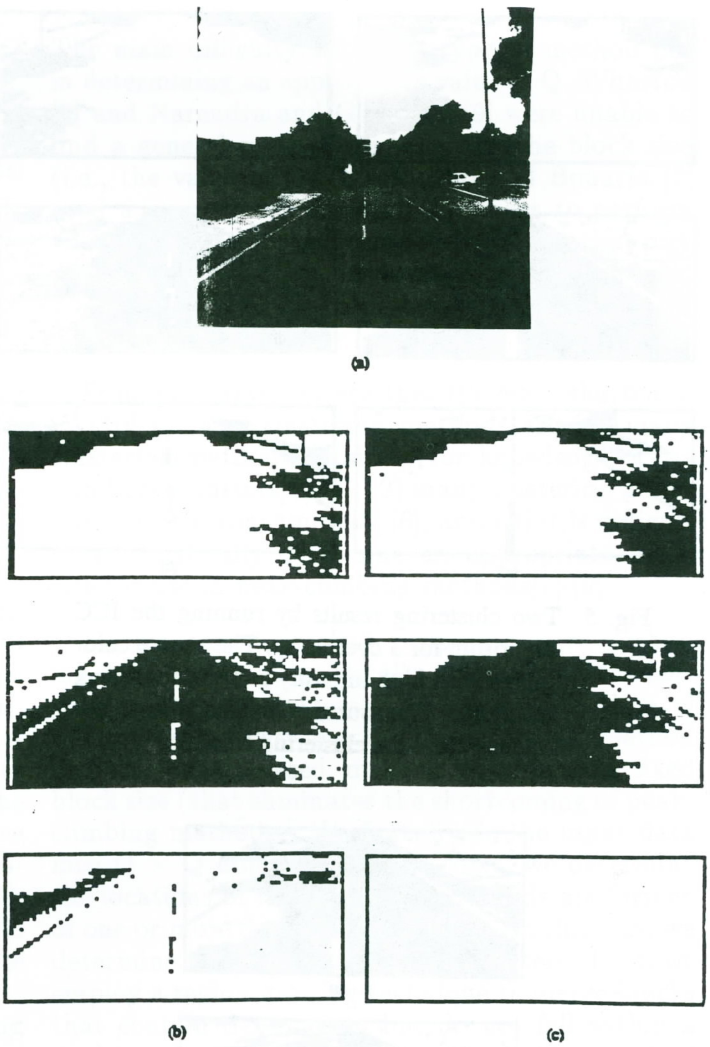

Fig. 4 The comparison between two clustering criteria based on different initial center choices after running for 3 cycles. (a). The source color image. (b). The result using the ICC algorithm. (c). The result using gray-level-averaging to set the initial centers to [0, 0, 0], [128, 128, 128], and [255, 255, 255].

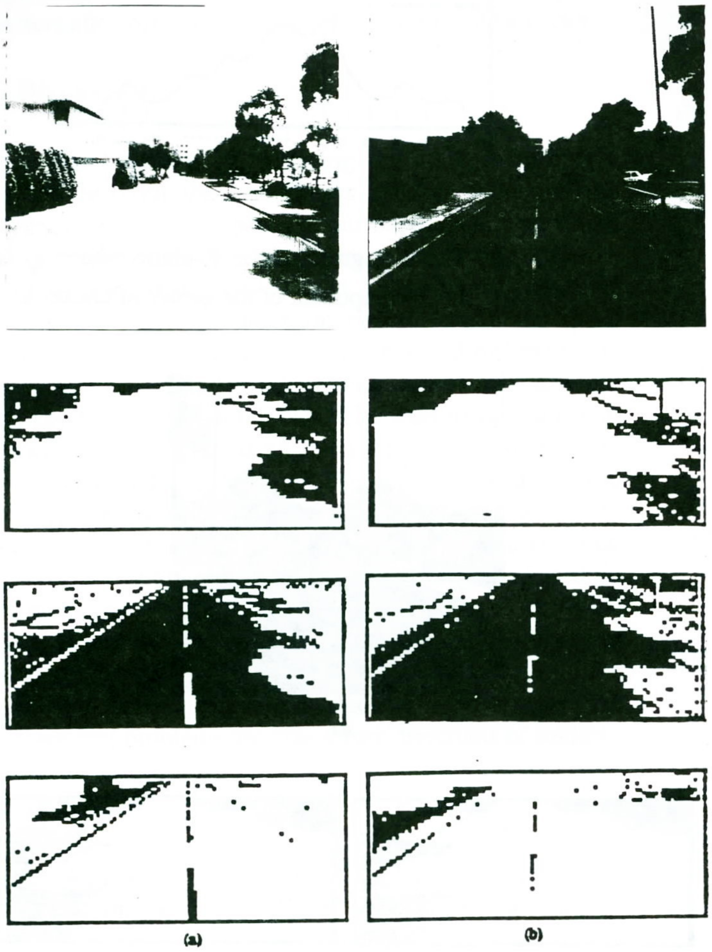

Fig. 5 Two clustering results by running the ICC algorithm for 3 cycles. (a). The source color image with high intensity and the clustering result. (b). The source color image with low intensity and the clustering result.

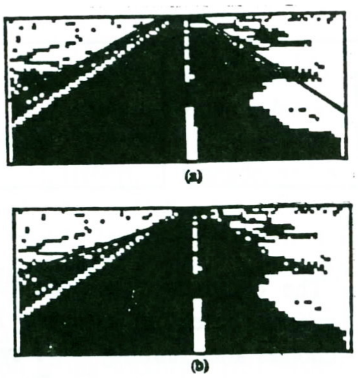

Fig. 6 Two matched road-templates represented by the red lines based on two different methods. (a). Result using MBPNM. (b). Result using MBPRM.

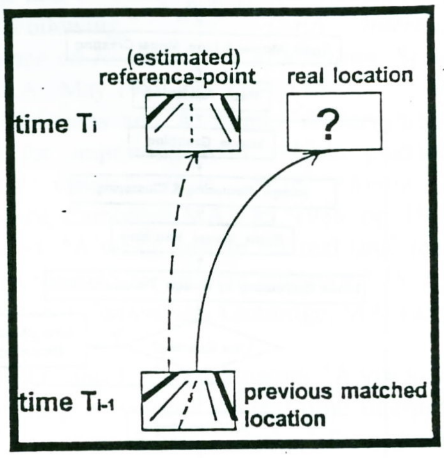

Fig. 7 The reference-point.

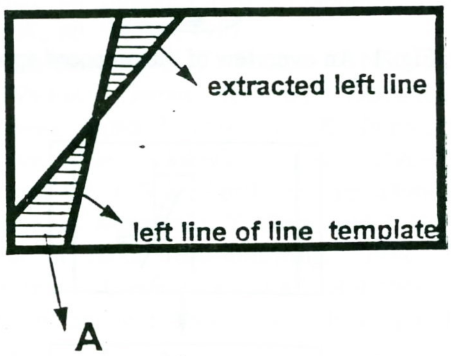

Fig. 8 The area A bounded by the extracted left line and the left line of the line-template.

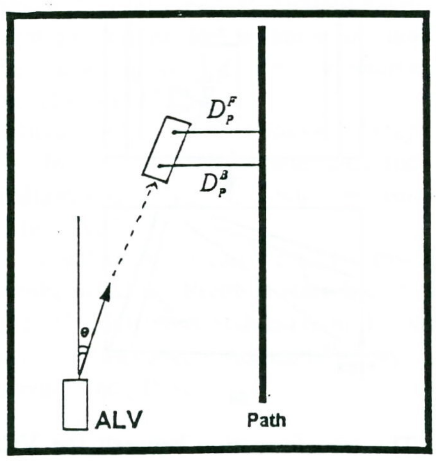

Fig. 9 A closeness distance measure $L_P(\delta) = \left(D_P^F\right)^2 + \left(D_P^B\right)^2$.